Chemical Science

ROYAL SOCIETY OF CHEMISTRY

EDGE ARTICLE

View Article Online
View Journal | View Issue

Cite this: *Chem. Sci.*, 2023, **14**, 2585

All publication charges for this article have been paid for by the Royal Society of Chemistry

Orthogonal, modular anion–cation and cation–anion self-assembly using pre-programmed anion binding sites†

Ayan Dhara,‡[ab] Rachel E. Fadler,‡[ac] Yusheng Chen,[a] Laura A. Köttner,[ad] David Van Craen,[ae] Veronica Carta[a] and Amar H. Flood *[a]

Subcomponent self-assembly relies on cation coordination whereas the roles of anions often only emerge during the assembly process. When sites for anions are instead pre-programmed, they have the potential to be used as orthogonal elements to build up structure in a predictable and modular way. We explore this idea by combining cation (M^+) and anion (X^-) binding sites together and show the orthogonal and modular build up of structure in a multi-ion assembly. Cation binding is based on a ligand (L) made by subcomponent metal-imine chemistry (M^+ = Cu^+, Au^+) while the site for anion binding (X^- = BF_4^-, ClO_4^-) derives from the inner cavity of cyanostar (**CS**) macrocycles. The two sites are connected by imine condensation between a pyridyl-aldehyde and an aniline-modified cyanostar. The target assembly [LM-**CS**-X-**CS**-ML],$^+$ generates two terminal metal complexation sites (LM and ML) with one central anion-bridging site (X) defined by cyanostar dimerization. We showcase modular assembly by isolating intermediates when the primary structure-directing ions are paired with weakly coordinating counter ions. Cation-directed (Cu^+) or anion-bridged (BF_4^-) intermediates can be isolated along either cation–anion or anion–cation pathways. Different products can also be prepared in a modular way using Au^+ and ClO_4^-. This is also the first use of gold(I) in subcomponent self-assembly. Pre-programmed cation and anion binding sites combine with judicious selection of spectator ions to provide modular noncovalent syntheses of multi-component architectures.

Received 13th September 2022
Accepted 20th January 2023

DOI: 10.1039/d2sc05121d

rsc.li/chemical-science

Introduction

The role of anions in cation-directed self-assembly is growing in importance. They act as templates[1–3] for coordination cages,[4] helicates[5] and knots,[6] triggers for switching between structures,[1,7,8] they solubilize[9] the final assembly in desired solvents, and get encapsulated as guests.[10] These many roles have grown on the back of metal-directed subcomponent self-assembly[11] involving the elegantly direct and *in situ* Schiff-base condensation of modular ligands. Across all these roles, the anion's binding site is built up dynamically by the cation-directed self-assembly[12–15] where metal ion coordination remains the primary structure-directing interaction. The anions have only rarely been explored as orthogonal motifs for building up structural features in a manner that matches metal ions. A notable exception[16] from Jansone-Popova is the synergistic one-pot self-assembly of a helicate around divalent metal cations, (Cu^{2+}) and sulfate anions (SO_4^{2-}) all directed by heteroditopic ligands composed of separate cation and anion binding sites. Herein, we investigate the orthogonality between anion coordination chemistry[17,18] and cation coordination for the modular build-up of ion-driven assemblies (Fig. 1).

The realization of structure-directing anion coordination is enabled by advances in receptor design.[19–23] Examples include anion helicates[24] with ditopic ligands bearing terminal ureas wrapped around phosphate (PO_4^{3-}).[25] Cages,[26] *e.g.*, tetrahedra, have combined urea motifs with highly charged phosphates in the vertices.[27] Polymers have been developed, *e.g.*, the Texas-sized box electrostatically stabilizes the polymerization of terephthalates,[28] and cyanostar stabilizes polymerization of diphosphonates[29] or diphosphates.[30] The counter cations in these cases, once again, play secondary roles.

Examples of multi-ion assemblies with anions and cations serving as equal partners are under-represented.[31–35] Ion-pair

[a]*Department of Chemistry, Indiana University, 800 East Kirkwood Avenue, Bloomington, IN 47405, USA. E-mail: aflood@indiana.edu*

[b]*Department of Chemistry and Biochemistry, University of Windsor, Windsor, Ontario, N9B 3P4, Canada*

[c]*Wayne State University Law School, Wayne State University 471 W Palmer Ave, Detroit, MI 48202, USA*

[d]*Department of Chemistry and Pharmacy, Friedrich-Alexander-Universität Erlangen-Nürnberg, Nikolaus-Fiebiger-Str. 10, 91058 Erlangen, Germany*

[e]*Department of Chemistry and Chemical Biology, Technische Universität Dortmund, Otto-Hahn-Str. 6, 44227 Dortmund, Germany*

† Electronic supplementary information (ESI) available. CCDC 2091810. For ESI and crystallographic data in CIF or other electronic format see DOI: https://doi.org/10.1039/d2sc05121d

‡ These authors contributed equally.

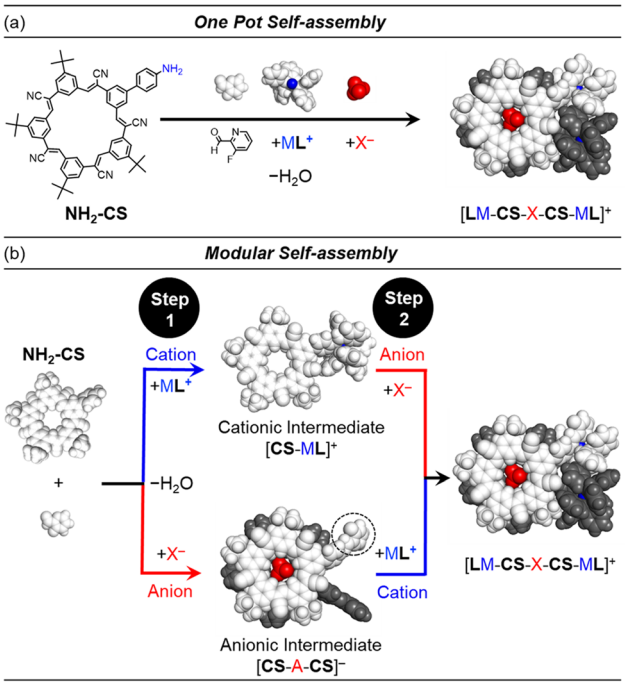

Fig. 1 Schematic summary of the (a) one-pot and (b) two-step self-assembly pathways that use pre-programmed and orthogonal coordination of cations and anions. In the resulting assembly (at right) the top cyanostar is shown in white and the bottom one is shown in dark grey for clarity. The Cu^+ cation is shown in blue, and the BF_4^- anion shown in red. The pyridyl-based aldehyde is highlighted by the dotted circle in the anionic intermediate.

receptors can bind cations, anions and ion pairs but such receptors are not used to build up structure unless both ions[36] bind at the same time to pre-formed metal and anion binding sites.[37] The most powerful among them afford cooperativity[38–40] with selective capture of ion pairs over the separate ions.[16] Such systems rely on one-pot processes with mutual binding of anion and cation without the isolation of intermediates for modular assembly.

Orthogonality between metal coordination and anion recognition offers advantages for self-assembly. When cation and anion do not interact either with each other or the other's binding sites then the assembly should be pre-programmable in a predictable way. Orthogonality also lends modularity. Thus, swapping one type of anion for another alters the composition but not the structural features of the final assembly. These characteristics of predictability and modularity can potentially be demonstrated by separating a one-pot multi-component self-assembly (Fig. 1a) into discrete steps (Fig. 1b).

Herein, we explore the orthogonality and modularity of ion-driven assembly by combining cation-directed subcomponent self-assembly between imines and metal moieties[42] (**ML**; **L** = **POP**, **PPh$_3$**; Fig. 2b) with pre-programmed anion binding sites (Fig. 2).[41] We use cyanostar macrocycles (**CS**, Fig. 2c)[22] for strong anion coordination (X^-, Fig. 2a). Structure-directing cations ($M = Cu^+$, Au^+; Fig. 2b) and anions ($X^- = BF_4^-$, ClO_4^-; Fig. 2a) can be added to form target assemblies in one-pot confirming the orthogonality of assembly. Modularity is demonstrated by first isolating supramolecular intermediates of either ion (Fig. 1b). The intermediates are accessed by using non-coordinating counterions (Fig. 2d and e). The cationic intermediate [**LCu-CS**]$^+$, and the anionic intermediate [**NH$_2$CS**-BF$_4$-**NH$_2$CS**]$^-$, can be

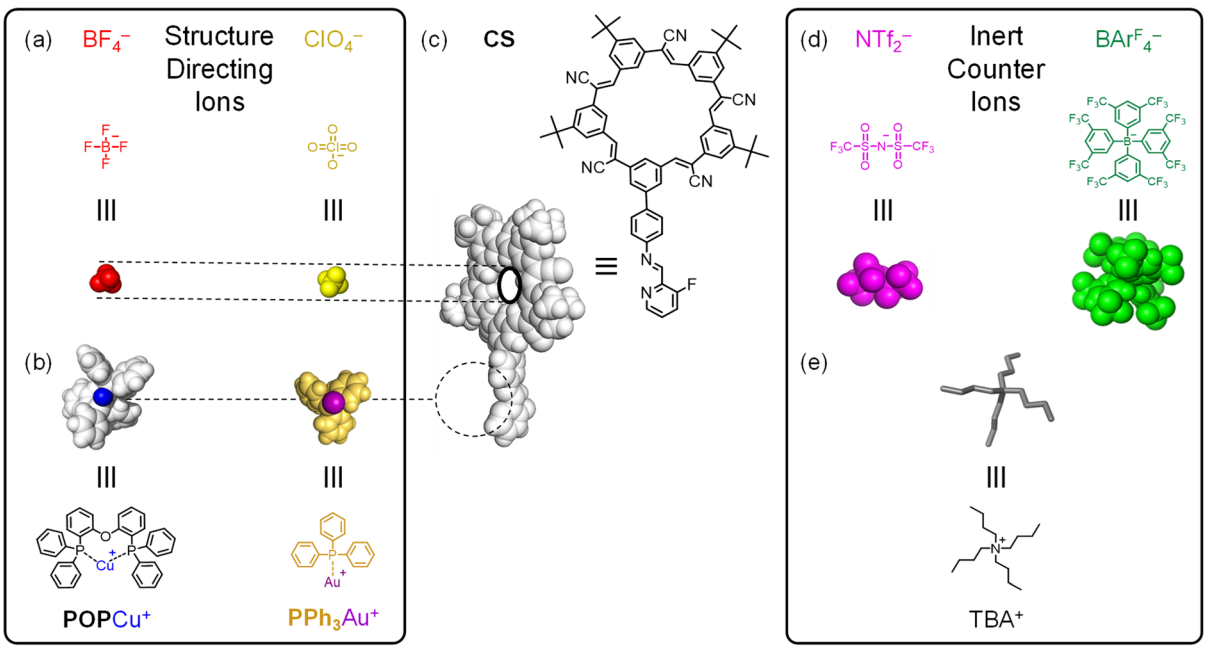

Fig. 2 Multi-component ion-directed self-assembly makes use of (a) structure-directing anions and (b) cations, (c) the pre-programmed anion-binding ligand, cyanostar (**CS**), as well as (d) inert counter anions and (e) counter cations. The Cu^+ is blue, and the Au^+ cation is dark purple. Their complexes are distinguishable by their ligands where POP is white and PPh_3 is gold. Anions are color-coordinated where BF_4^- is red, ClO_4^- is yellow NTf_2^- is purple, and $BArF_4^-$ is green.

isolated by trituration and used in subsequent reactions. Exemplary studies with copper(I) and tetrafluoroborate indicate the intermediate can be used as a substrate for a second coordination step to form the final assembly [**L**Cu-**CS**-BF_4-**CS**-Cu**L**],$^+$ (Fig. 1b). Modularity was also demonstrated using Au^+ and ClO_4^- ions. Surprisingly, this is the first example of subcomponent self-assembly[43] with Au(I). We used other anions (phosphates, phosphonates, bisulfate) to explore the limits of this strategy. Thus, pre-programmed cation and anion binding sites serve as orthogonal interactions that form supramolecular assemblies and help contribute to the growing exploration of methods[44,45] capable of orthogonal, modular noncovalent synthesis.

Results and discussions

Design of the components used in cation–anion self-assembly

In order to demonstrate orthogonality, we needed to simplify the number of potential products that form. We used ancillary ligands on the metals to block the possibility of cross linking. We substituted just one of the five cyanostar arms (Fig. 1a) to enable coordination of one metal ion moiety to the macrocycle as opposed to five in the C_5-symmetric cyanostar. The only drawback to mono-substitution is the presence of overlapping peaks in the NMR spectra. These ligand and receptor features all favor formation of fewer species.

We used knowledge of the recognition patterns of the binding sites to design the various components.[42] The mono-substituted cyanostar[46] (**NH_2-CS**, Fig. 1) contains a 4-aminophenyl group. We expect this aniline to enable imine formation upon reaction with aldehydes in the presence of metal ions.[43] We also anticipate anion coordination with **NH_2-CS** will match the behavior of parent cyanostar (**pCS**)[22] to direct formation of a 2 : 1 sandwich complex with a bridging anion, X^-. For metal complexation, we selected a fluoro-substituted picolinaldehyde, **F-PyCHO**, as the partner to the **NH_2-CS** aniline for subcomponent assembly.

We identified two metal precursors to explore modularity. The copper(I) complex of bis(2-(diphenylphosphino)phenyl) ether (**POP**) as the bis-acetonitrile solvato species, {**POP**Cu$(MeCN)_2$}$^+$, was selected as the first. The **POP** ligand is known to terminate the assembly after imine coordination[42] and the acetonitrile is labile. The second is a gold(I) triphenylphosphine moiety, {**PPh_3**Au}$^+$. Gold(I) has never been used in subcomponent self-assembly and it has unique coordination geometries.[47] Gold(I) is typically two coordinate,[48] but three has also been observed when using σ-donors of comparable strength.[49] The imine nitrogen is a relatively strong donor,[50] therefore a two-coordinate geometry is possible. Alternatively, the chelating imine is similar to phenanthroline that can favor three-coordinate geometries with gold(I).[51] A model gold(I) complex was examined to confirm the preferred mode of coordination prior to the cation–anion self-assembly.

Strategies for orthogonal cation–anion self-assembly

Our strategy for demonstrating the principle of cation and anion self-assembly relies on two design principles: orthogonal binding sites and weak ion-pair interactions. The cyanostar component has an anion-binding site native to its cavity and one cation binding site added to its exterior. Based on their preferred reactivity,[22,42] these sites do not compete with each other. The second criterion requires knowledge of ion coordination and ion pairing. Copper(I) ions are known to coordinate with free imines while BF_4^- is complementary to the cyanostar. These ions (Cu^+ and BF_4^-) do not display strong interactions with each other in the solvents we use here.[52] While BF_4^- anions are considered weakly coordinating to metals, they display some of the strongest binding affinities to cyanostar.[22] But not all anions that bind tightly to cyanostar are inert to metal coordination (see below). These design principles are anticipated to be transferrable to other pairs of ions. To this end, we investigated gold(I), Au^+, and perchlorate, ClO_4^- to verify the generality of this assembly strategy.

Finally, isolation of intermediates requires selection of non-binding counter ions. Their use enables structure-directing ions to be delivered separately and sequentially. Bulky anions tetrakis(3,5-bis(trifluoromethyl)phenyl)borate ($BAr^F{}_4^-$, Fig. 2d) and triflimide (NTf_2^-, Fig. 2d) fulfill the requirements for weak counter anions. They are well-established to coordinate poorly to both metal ions[53,54] and cyanostar.[55] NTf_2^- has a low affinity ($250 \pm 30\ M^{-1}$) for cyanostar.[52] Similarly, the TBA^+ counter cation (tetrabutylammonium, Fig. 2e) is not known to coordinate to metal-binding ligands. While the ion pairing of TBA^+ in dichloromethane with our target anions, *e.g.* BF_4^- $\log K = 4.6$ (ref. 56) and ClO_4^- $\log K = 4.24$ (ref. 57) is not negligible, they are weaker than the coordination with parent cyanostar, *e.g.*, $\log \beta$(**pCS**-ClO_4^--**pCS**) ~12.[22] Thus, any ion pairing does not interfere.

One-pot, multi-component self-assembly using Cu^+-coordination and cyanostar-BF_4^- binding

Orthogonality between the two binding sites was verified using a traditional one-pot assembly. The structure-directing Cu^+ and BF_4^- ions can be added as a single precursor (Fig. 3a). The target assembly [**POP**Cu-**CS**-BF_4-**CS**-Cu**POP**]$^+$, is a dicopper and anion-bridged dimer. The copper binding sites are products of imine condensation between **NH_2CS** and **F-PyCHO** in the presence of the salt [**POP**Cu$(MeCN)_2$]·BF_4. Mixtures of the three components proceed near-quantitatively through to the target assembly. The product was isolated as a BF_4^- salt after solvent removal. Exploration of the assembly conditions revealed that excess aldehyde enhanced the yield and unreacted aldehyde could be removed with ether washes. Excess **NH_2CS** was not investigated on account of its poorer solubility relative to the aldehyde.

Product identity was confirmed using NMR spectroscopy and electrospray ionization mass spectrometry (ESI-MS). The well-resolved ^{1}H NMR peaks (Fig. 3b) indicate high-fidelity Cu(I)-complexation and BF_4^- binding in the target assembly. Diffusion ordered spectroscopy (DOSY, Fig. 3b) verified formation of a single monodisperse species. ESI-MS shows the peak for the parent assembly [**POP**Cu-**CS**-BF_4-**CS**-Cu**POP**]$^+$ at 3407.2455 *m*/*z* (Fig. 3c). Under ESI-MS conditions, minor multimer peaks are

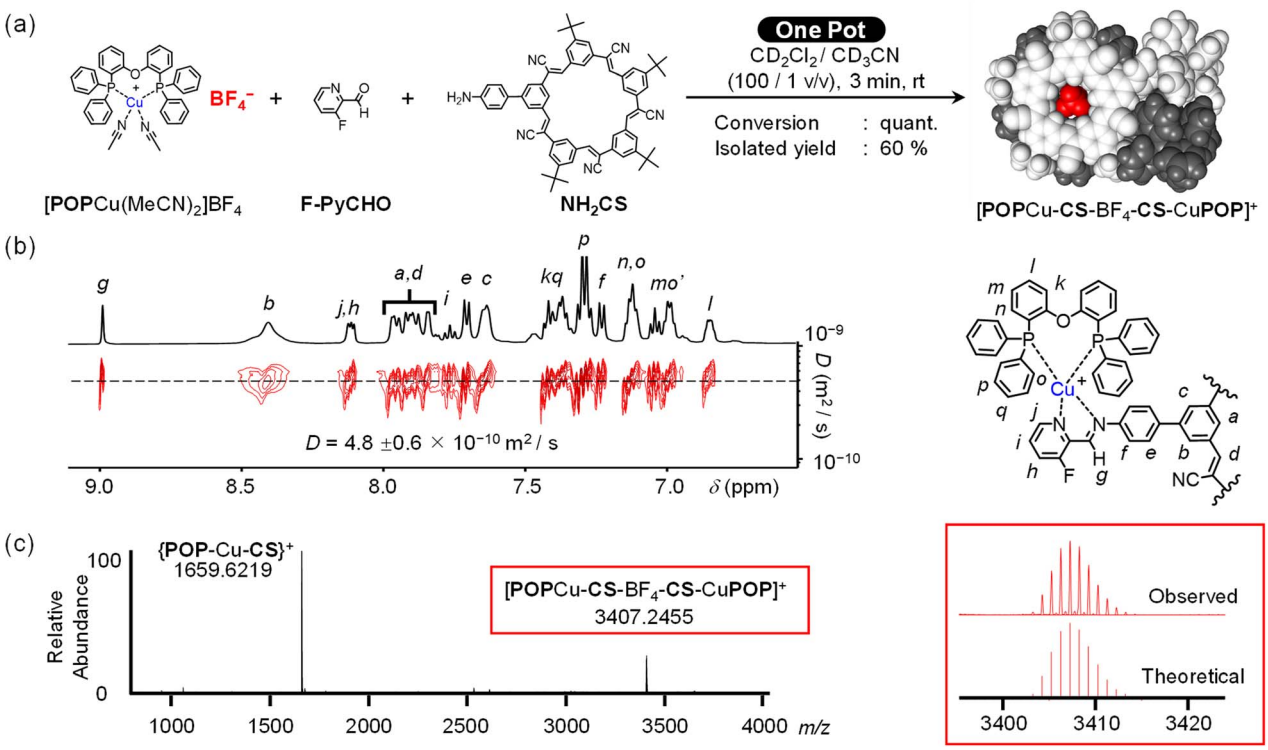

Fig. 3 (a) One-pot reaction to form [**POP**Cu-**CS**-BF_4-**CS**-Cu**POP**]$^+$ and characterization by (b) DOSY NMR (CD_2Cl_2, 2 mM), and (c) ESI-MS spectrum of assembly (CH_2Cl_2, 2 mM).

observed from 0.5 Dalton peak-to-peak separation associated with a dimer of the target: [**POP**Cu-**CS**-BF_4-**CS**-Cu**POP**]$_2^{2+}$. We also see a daughter peak corresponding to the anion-free half of the assembly assigned to the {**CS**-Cu**POP**}$^+$ moiety at 1659.6219 *m*/*z*.

Imine formation and metal coordination show characteristic changes in the chemical shifts of key protons upon formation of the target assembly (Fig. S53†). The aldehyde (10.16 ppm) is consumed to form the imine (9.01 ppm).[58] Other proton close to the metal binding site are characteristic of imine bond formation and copper complexation.[42] The aniline's ring hydrogen (H_f, 6.84 ppm) shifts downfield (7.23 ppm), and the phosphine protons (H_k) shift modestly from 7.02 to 7.09 ppm.

Anion binding in the target assembly is confirmed by ^{1}H NMR (Fig. S53†). Peak assignments were based on ROESY studies, controls, and assignments of a related cyanostar.[21] The cluster of peaks at 8.76 ppm in **NH$_2$CS** are assigned to the outer H_b protons of the macrocycle. After one-pot assembly, these shift upfield to 8.41 ppm matching the parent cyanostar.[22] The ^{19}F NMR signal from BF_4^- shows a single broad peak at −150 ppm (Fig. 4a) consistent with exchange averaging between complexed and outer-sphere ions.[59] The spectrum of BF_4^- as a TBA^+ salt shows a sharp peak at −152 ppm (Fig. 4c) while the 2 : 1 complex formed between BF_4^- and the parent cyanostar (Fig. 4b) resonates as a sharp peak at −148 ppm.

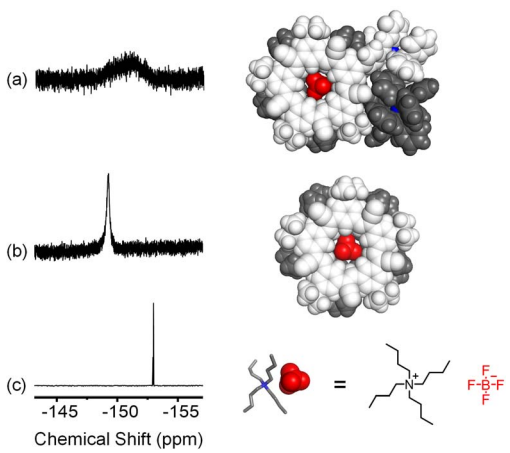

Fig. 4 ^{19}F NMR (a) [**POP**Cu-**CS**-BF_4-**CS**-Cu**POP**]$^+$ created in one-pot, (b) [**pCS**-BF_4-**pCS**]$^-$, and (c) $TBABF_4$ in CD_2Cl_2 (298 K, 376 MHz).

Cation-directed supramolecular intermediates

Formation of the desired multi-component assembly [**POP**Cu-**CS**-BF_4-**CS**-Cu**POP**]$^+$, in one pot (Fig. 1a) with high yields provides a basis for exploring stepwise synthetic strategies (Fig. 1b). We separately investigated generation of cation-directed and anion-directed intermediates by relying on their pre-programmed binding sites. In traditional cation-directed assembly, it is not possible to isolate the anion-directed intermediates because the anion binding site is built *in situ* instead of being pre-programmed.

The cation-directed supramolecular intermediate was prepared under similar conditions as the one pot but using the

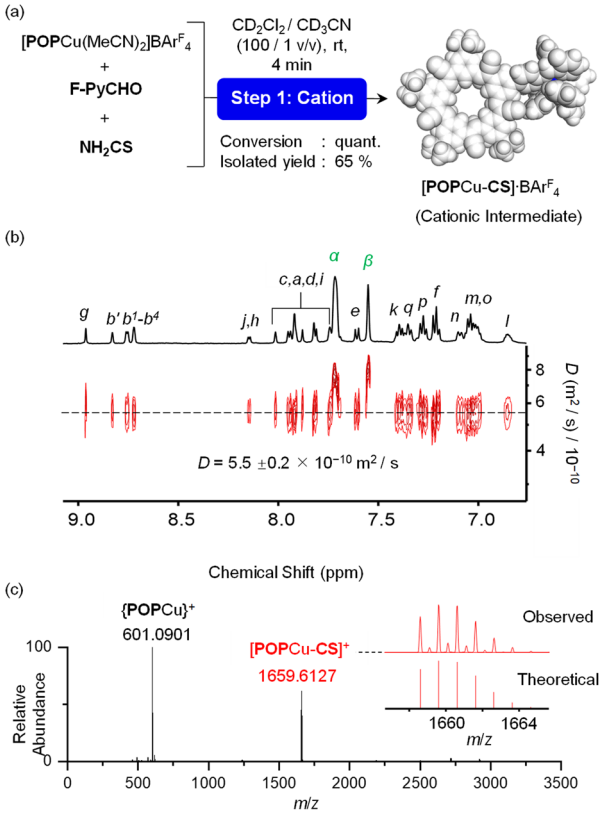

Fig. 5 (a) Reaction to form [**POP**Cu-**CS**]$^+$ and characterization by (b) DOSY NMR (CD_2Cl_2, 2 mM), and (c) ESI-MS spectrum (CH_2Cl_2, 2 mM).

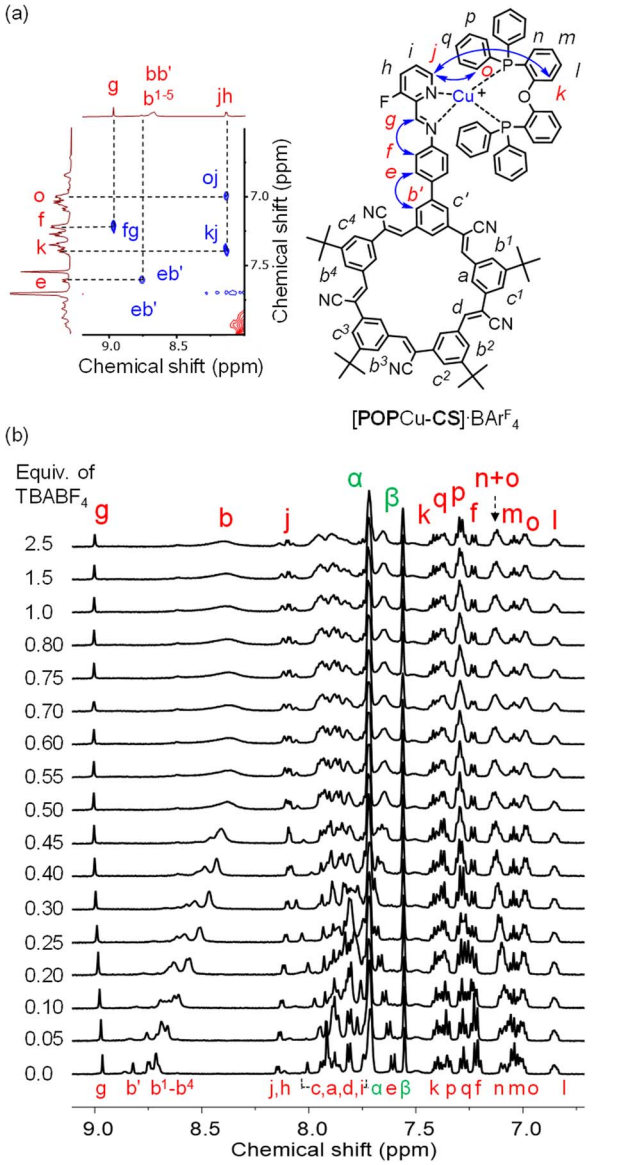

Fig. 6 (a) The aromatic region of ROESY NMR data of [**POP**Cu-**CS**]·BAr^F_4. (b) ^{1}H NMR titration of [**CS**-**POP**Cu]·BAr^F_4 (2 mM) with $TBABF_4$ (CD_2Cl_2, 400 MHz, rt).

copper precursor [**POP**Cu(MeCN)$_2$]$^+$ as a $BAr^F_4{}^-$ salt (Fig. 5a). Identification of the desired monomeric intermediate [**POP**Cu-**CS**]$^+$ was obtained from the ESI-MS with a peak at 1659.6127 *m*/*z* (Fig. 5c). DOSY confirmed formation of a single monodisperse species (Fig. 5b). Characteristic shifts in NMR peaks confirm formation of intermediate [**POP**Cu-**CS**]$^+$ (Fig. S54†). The $BAr^F_4{}^-$ anion peaks are unshifted indicative of its innocence. ROESY data (Fig. 6) on the intermediate confirms imine formation and {**POP**Cu}$^+$ complexation.

Modular synthesis using a universal cation-directed supramolecular intermediate with different anions

Preparation of the cationic intermediate [**POP**Cu-**CS**]$^+$ allowed investigation of different anion-driven products with $BF_4{}^-$ or $ClO_4{}^-$ (Fig. 6 and 7) to illustrate modularity. Addition of $TBABF_4$ to [**POP**Cu-**CS**]$^+$ led to the cyanostar-mediated dimerization around the bridging $BF_4{}^-$ anion. ^{1}H NMR titration monitoring addition of $TBABF_4$ (Fig. 6b) to [**POP**Cu-**CS**]$^+$ indicate formation of a 2 : 1 complex with saturation at 0.5 equivalents (Fig. 6b). Diffusion NMR confirmed formation of a single monodisperse species (Fig. S62†). The dimeric assembly [**POP**Cu-**CS**-BF_4-**CS**-Cu**POP**],$^+$, was verified using ESI-MS (Fig. 7a) matching the one prepared by the one-pot method (Fig. 3c). A peak at 2533.9194 *m*/*z* indicates formation of a higher-order trimer [(**POP**Cu-**CS**)$_3BF_4$]$^{2+}$ only under the ESI-MS conditions.[20,29,30,57,60]

Consistent with the modularity of the cation–anion method, addition of $TBAClO_4$ generated the same types of signatures as those seen with $BF_4{}^-$. The dimeric assembly was seen by ESI-MS (Fig. 7b) with the same daughter and higher-order peaks. The diffusion coefficient matched the ones seen using the $BF_4{}^-$ anion (Fig. S63†). The ^{1}H NMR titrations also showed saturation at the expected 0.5 equivalence point $TBAClO_4$ (Fig. 7c).

Stepwise synthesis using anion-linked intermediates

The function of the pre-programmed anion binding site can be demonstrated by inverting the ion addition sequence using an anion–cation pathway. The anion-linked supramolecular intermediate [**CS**-BF_4-**CS**]$^-$ (Fig. 8) was created by condensation of 2 equivalents each of **NH$_2$-CS** and aldehyde **F-PyCHO** in the presence of 1 equivalent of $TBABF_4$. The ESI-MS analyses showed the intermediate (Fig. S14†) present as a variety of

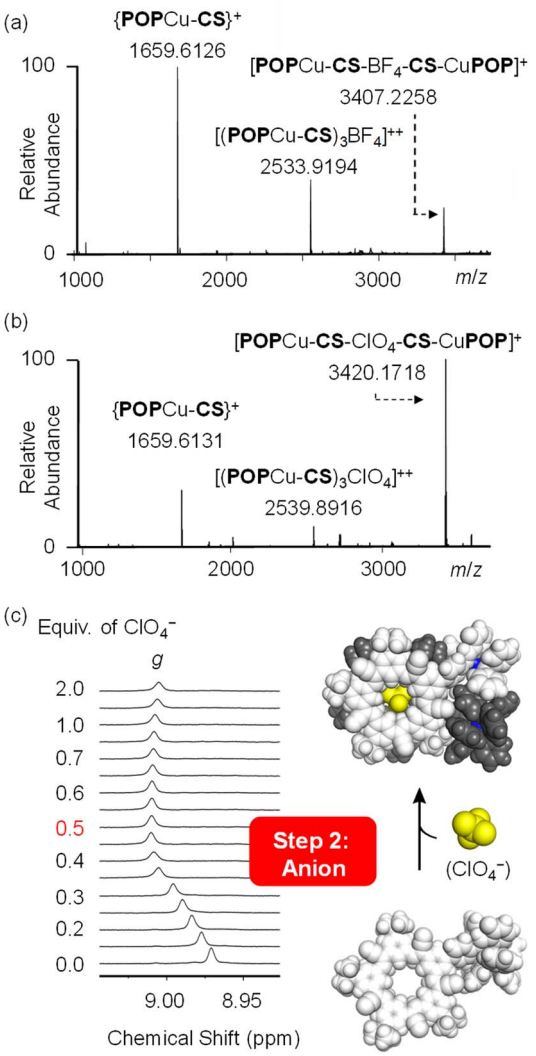

Fig. 7 ESI-MS spectra (CH_2Cl_2, 0.5 mM) of (a) [**POP**Cu-**CS**-BF_4-**CS**-Cu**POP**]$^+$ and (b) [**POP**Cu-**CS**-ClO_4-**CS**-Cu**POP**]$^+$ formed by cation–anion pathway. (c) ^{1}H NMR titrations of intermediate [**CS**-**POP**Cu]·$BAr^F{}_4$ (2 mM) with TBAClO_4 (CD_2Cl_2, 400 MHz, rt).

MeOH adducts under the conditions of the experiment. The 1 : 4 ratio seen by NMR between the free aldehyde (**F-PyCHO**) and the imine suggests 80% reaction. Metal-ion chelation is required to drive complete condensation.

Addition of [**POP**Cu$(MeCN)_2$]$^+$ in the second step (Fig. 8) drove complete formation of the imine and the target assembly,

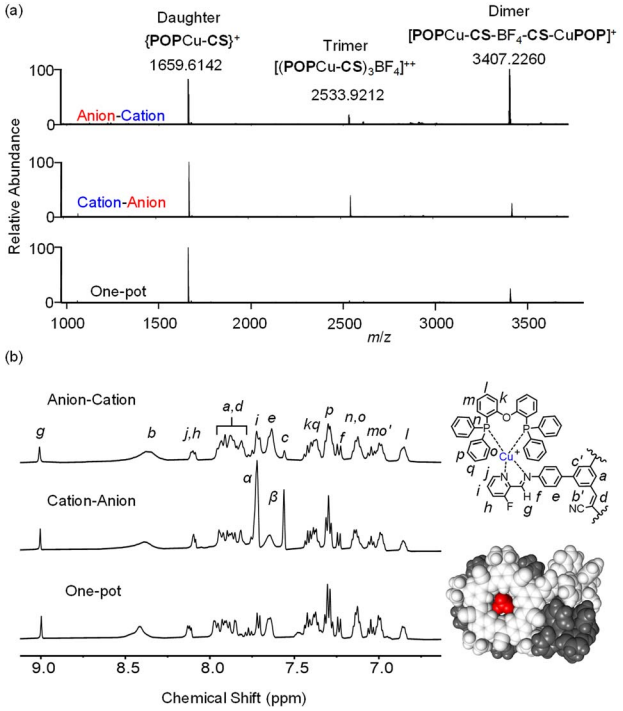

Fig. 9 (a) ESI-MS (CH_2Cl_2, 0.5 mM) and (b) diagnostic ^{1}H NMR peaks (CD_2Cl_2, 0.5 mM) for [**POP**Cu-**CS**-BF_4-**CS**-Cu**POP**]$^+$ for the anion–cation stepwise, cation–anion stepwise, and one-pot assembly.

[**POP**Cu-**CS**-BF_4-**CS**-Cu**POP**]$^+$. Notably, the product of the anion–cation assembly pathway shows the same diagnostic signatures in ESI-MS and NMR (Fig. 9) as the products of the one-pot and cation–anion methods confirming the same structure is made along three different synthetic pathways. The nature of the counter anions depends on the pathway used for self-assembly. In the cases where more than one counter anion is present, they are in exchange with the various species present in solution. For example, the ^{19}F NMR spectrum of the gold assembly obtained *via* the cation–anion pathway shows two peaks. One results from BF_4^- in fast exchange between being its cyanostar-bound and unbound states while the other corresponds to the uncomplexed NTf_2^- anion (Fig. S30†).

Orientation of the macrocycles in the dimer

Structurally, the copper complexes in the product [**POP**Cu-**CS**-BF_4-**CS**-Cu**POP**]$^+$ can be either *syn*, *meta*, or *anti* (Fig. 10).

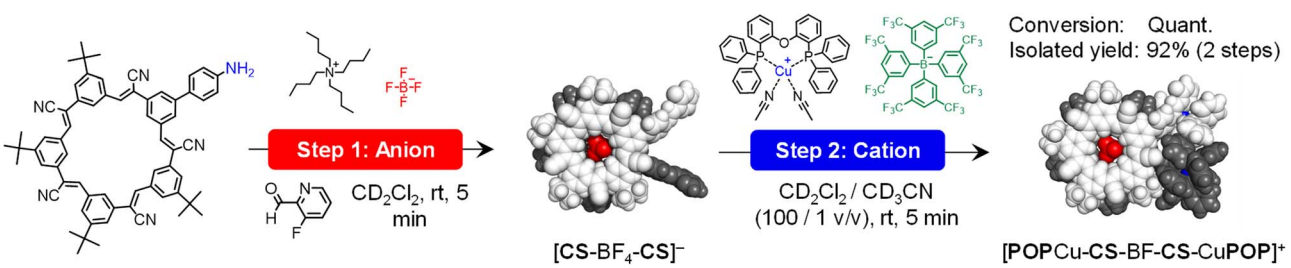

Fig. 8 Stepwise anion–cation synthesis.

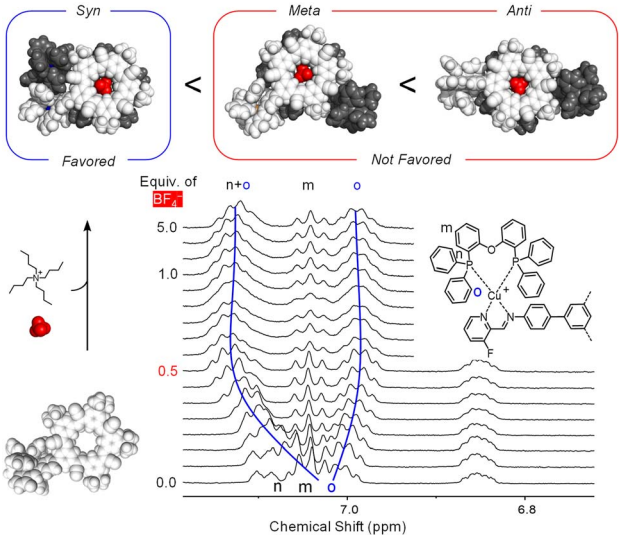

Fig. 10 ^{1}H NMR titration of $TBABF_4$ into [**POP**Cu-**CS**]$^+$ (4 mM) in CD_2Cl_2 (298 K, 400 MHz).

Molecular mechanics shows *syn* to be favored over *meta* (16 kJ mol^{-1}) and *anti* (86 kJ mol^{-1}), which is consistent with a related complex.[46] An NMR titration following addition of BF_4^- to [**POP**Cu-**CS**]$^+$ to form the dimerized product [**CuCS**-BF_4-**CSCu**]$^+$ supports the *syn* geometry. Therein, the phosphine ligands are close enough to lower their symmetry into two different environments (H_o, Fig. 10). Molecular models on the *syn* geometry how one of the two phenyls engaging in π stacking. These findings suggest the *syn* geometry is favored by stabilizing contacts between coordinated **POP** ligands.

Use of gold(I) showcases modularity of cation-directed supramolecular intermediates

Gold(I) was used to investigate the modularity of assembly. To model the first use of gold(I) ions in subcomponent self-assembly, we prepared a complex using a simple aniline. We mixed a gold(I) precursor as a triflimide salt, [**PPh$_3$**Au]·NTf_2 with **F-PyCHO** and the aniline *p*-toluidine. X-ray diffraction studies showed formation of tricoordinate gold(I) cation (Fig. 11) with a chelating imine. ^{1}H and ^{19}F NMR, and ESI-MS spectra (Fig. S36–S38†), are consistent with formation of the gold(I) complex seen in the solid state.

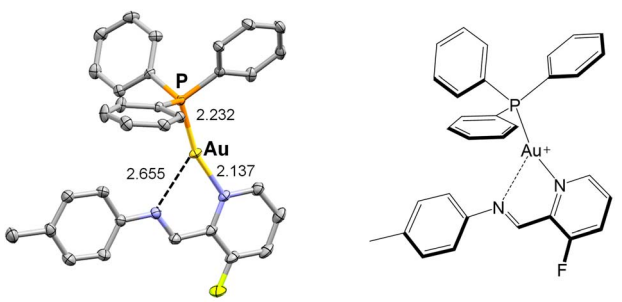

Fig. 11 Molecular structure of the three-coordinate gold(I) model complex as determined by X-ray crystallography (50% ellipsoids). Hydrogen atoms and counter anion omitted for clarity.

We examined the various synthetic pathways using the Au^+ and BF_4^- ions. The target complex [PPh_3Au-**CS**-BF_4-**CS**-AuPPh_3]$^+$ was formed along both one-pot and cation–anion pathways (Fig. 12a). Formation was confirmed by ESI-MS with the one-pot producing a peak at 3122.1669 *m*/*z* (Fig. S25†) matching the product of cation–anion assembly (Fig. 12b). Consistent with gold(I) complexes being less stable than copper(I), parent ion peaks have lower intensity than daughter ions.

Formation of the target assembly [**PPh$_3$**Au-**CS**-BF_4-**CS**-Au**PPh$_3$**]$^+$, was verified by NMR. All resonances display the same diffusion coefficients (Fig. 12c) for the one-pot and cation–anion assembly (Fig. S69†) and the same diagnostic peaks by ^{1}H-NMR (Fig. 13) and ^{19}F-NMR spectroscopy (Fig. S27†). These similarities indicate that the same assembly is being produced along different pathways.

The anion–cation stepwise pathway was also investigated. Using the anion-linked intermediate described earlier, addition of the Au^+ precursor produced an ^{1}H NMR spectrum differing from the one-pot and cation–anion pathways (Fig. S56†). The ESI-MS did not show any peaks consistent with target assembly. Adding excess BF_4^- to better match the one-pot pathway did not influence the outcome (Fig. S41†). Failure to access the target assembly by the alternative stepwise pathway is surprising and highlights the need to study the impacts of reaction order on multi-component supramolecular assemblies.

Failure modes using competitive anions

Not every anion that binds tightly to cyanostar[29,57,60,61] is also weakly coordinating to metal cations. We were hoping to leverage this idea to target assemblies that could only be produced by pre-complexation of the anion. To explore this idea, we studied how metal complexes survived in the presence of organophosphates, which are known to ligate metals. These phosphates are also known to form threaded pseudorotaxane complexes with cyanostar.[62] This study was undertaken using gold and copper complexes, dibutyl phosphate, dibenzyl phosphate, and the parent cyanostar, **pCS**, as models. However, pre-complexation with cyanostar did not prevent the phosphates from decomposing the copper complexes in 24 hours (Fig. S71–S75†). A gold complex showed similar behavior (Fig. S76 and S77†) as did the cationic intermediate [**PPh$_3$**Au-**CS**]·NTf_2 (Fig. S77†). While we saw some evidence of a threaded pseudorotaxane, the ^{1}H NMR spectra suggests that the phosphate binds to the gold ions in the complex as opposed to the cyanostar cavity (Fig. S71†). In addition, the bisulfate (HSO_4^-)[57,60] and *n*-hexylphosphonate ($C_6H_{13}PO_3H^-$)[29] anions that can drive cyanostar dimerization, behaved poorly and stripped copper ions off the complex (Fig. S71–S75†). An instantaneous loss of color was indicative of decomplexation.

Hence, testing the orthogonality of the ion interactions involved in the noncovalent bond forming reactions and verifying the compatibility of the ions with each other is a key step for successful implementation of ion-by-ion stepwise self-

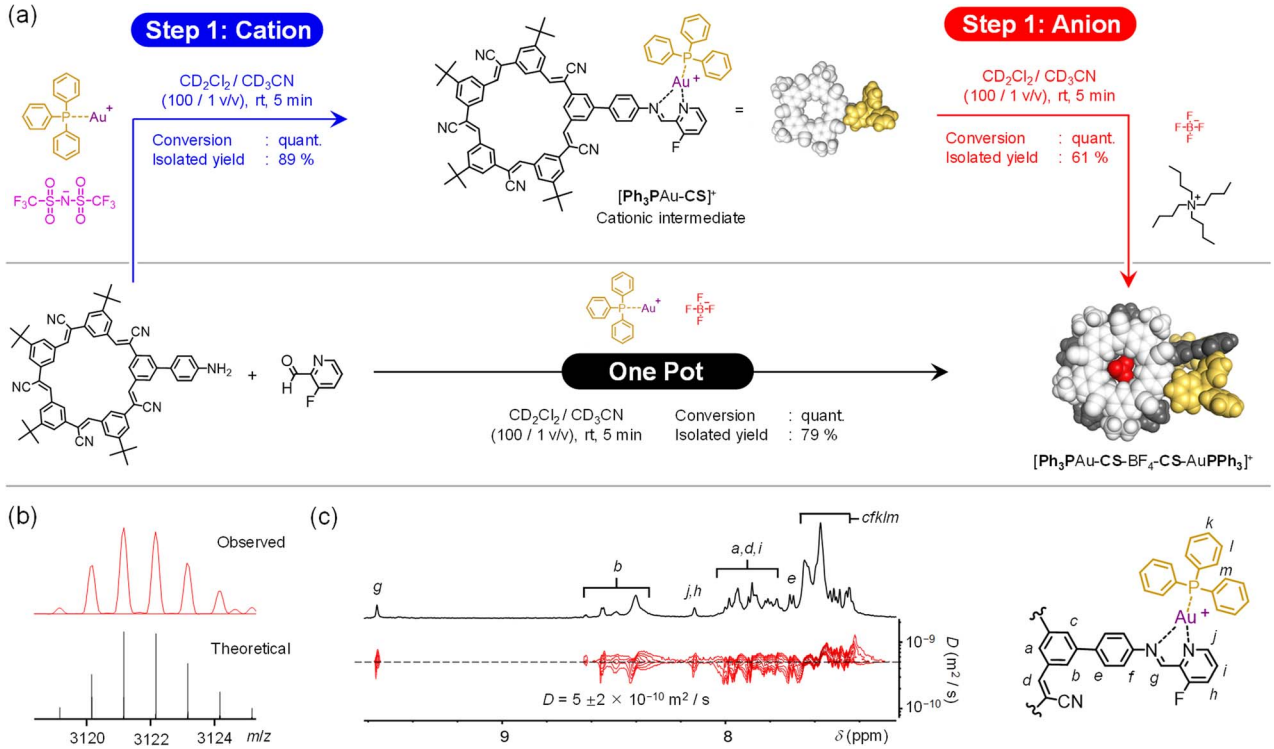

Fig. 12 (a) Reactions to form [PPh_3Au-CS-BF_4-CS-AuPPh_3]$^+$ by one-pot and cation–anion pathways. (b) ESI-MS (CH_2Cl_2, 0.5 mM) of [PPh_3Au-CS-BF_4-CS-AuPPh_3]$^+$ prepared *via* cation–anion pathway. (c) DOSY NMR (CD_2Cl_2, 2 mM) of [PPh_3Au-CS-BF_4-CS-AuPPh_3]$^+$ created in one-pot assembly.

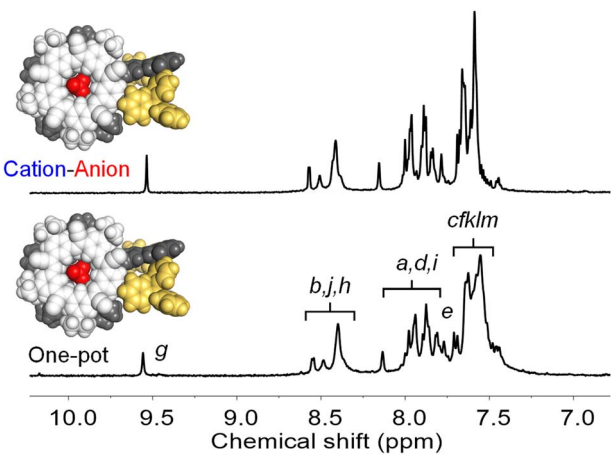

Fig. 13 Diagnostic ^{1}H NMR peaks (CD_2Cl_2, 0.5 mM) for [PPh_3Au-CS-BF_4-CS-AuPPh_3]$^+$ obtained by one-pot assembly and cation–anion assembly.

assembly. Use of cyanostar as a supramolecular element[41] with its strong affinity for anions known to weakly coordinate with metals may be key to this demonstration suggesting other receptors, like bambusuril,[63–66] may also be used in this way.

Conclusion

We demonstrated that orthogonal cation–anion and anion–cation self-assembly can be used to build up the structures of multi-component assemblies in a modular manner by using pre-programmed binding sites for both cations and anions. This orthogonal ion-by-ion strategy of subcomponent self-assembly enables similar structures to be accessed in a modular manner using common intermediates in both a one-pot and stepwise way. The architectures involved Cu(I) and Au(I) complexes situated on the termini of the anion-driven cyanostar dimers form [**POP**Cu-**CS**-X-**CS**-Cu**POP**]$^+$ and [PPh_3Au-CS-X-CS-AuPPh_3]$^+$, where the bridging anion (X) can be either BF_4^- or ClO_4^-. We find that the noncovalent chemistries of anion and cation coordination can be readily paired with the covalent chemistry of sub-component self-assembly based on modular imine-based ligands. The combination of anion receptors with established ligands for metal complexation introduce a new approach to design architectures based on orthogonal cation–anion self-assembly.

Data availability

The ESI is available free of charge on the journal website. General methods, NMR titrations, 2D NMR spectroscopy, X-ray diffraction analyses, and ESI-MS analyses.

Author contributions

AD conceived the project under the supervision of AHF; in response to the Covid pandemic, REF assisted AHF with overseeing project completion. AD conducted experiments with

assistance from LAK, YC, REF, DVC and VC; AD designed, created and characterized the assemblies with initial input from LAK; YC, REF and LAK made and characterized compounds and collected control data; DVC grew a single crystal and VC collected X-ray diffraction data, solved and refined the crystal structure; AD, REF and AHF analyzed the data, wrote and edited the manuscript with input from all co-authors.

Conflicts of interest

The authors declare no competing financial interests.

Acknowledgements

We acknowledge support from the National Science Foundation (CHE 2105848). We thank Xinfeng (Frank) Gao at Indiana University Bloomington for his help with NMR spectroscopy. The 500 MHz NMR spectrometer of the Indiana University NMR facility was supported by NSF grant CHE-1920026 and the Prodigy probe was purchased in part with support from the Indiana Clinical and Translational Sciences Institute funded, in part by NIH Award TL1TR002531. Support for the acquisition of the Bruker Venture D8 diffractometer through the Major Scientific Research Equipment Fund from the President of Indiana University and the Office of the Vice President for Research is gratefully acknowledged. REF thanks the Raymond Siedle Materials Fellowship for support and the National Institutes of Health (T32 GM109825) for support through the training grant entitled "Graduate Program in Quantitative and Chemical Biology at Indiana University Bloomington". We thank the staff of the Indiana University Mass Spectrometry Facility for recording mass spectra and accommodating high-concentration samples.

Notes and references

1 I. A. Riddell, M. M. J. Smulders, J. K. Clegg, Y. R. Hristova, B. Breiner, J. D. Thoburn and J. R. Nitschke, Anion-induced reconstitution of a self-assembling system to express a chloride-binding Co10L15 pentagonal prism, *Nat. Chem.*, 2012, **9**, 751–756.

2 L. H. Foianesi-Takeshige, S. Takahashi, T. Tateishi, R. Sekine, A. Okazawa, W. Zhu, T. Kojima, K. Harano, E. Nakamura, H. Sato and S. Hiraoka, Bifurcation of self-assembly pathways to sheet or cage controlled by kinetic template effect, *Commun. Chem.*, 2019, **1**, 128.

3 R. Zhu, J. Lübben, B. Dittrich and G. H. Clever, Stepwise Halide-Triggered Double and Triple Catenation of Self-Assembled Coordination Cages, *Angew. Chem., Int. Ed.*, 2015, **9**, 2796–2800.

4 I. A. Riddell, M. M. Smulders, J. K. Clegg, Y. R. Hristova, B. Breiner, J. D. Thoburn and J. R. Nitschke, Anion-induced reconstitution of a self-assembling system to express a chloride-binding Co10L15 pentagonal prism, *Nat. Chem.*, 2012, **9**, 751–756.

5 C. J. Massena, D. A. Decato and O. B. Berryman, A Long-Lived Halogen-Bonding Anion Triple Helicate Accommodates Rapid Guest Exchange, *Angew. Chem., Int. Ed.*, 2018, **49**, 16109–16113.

6 D. A. Leigh, R. G. Pritchard and A. J. Stephens, A Star of David catenane, *Nat. Chem.*, 2014, **11**, 978–982.

7 A. I. Share, K. Parimal and A. H. Flood, Bilability is Defined when One Electron is Used to Switch between Concerted and Stepwise Pathways in Cu(I)-Based Bistable [2/3] Pseudorotaxanes, *J. Am. Chem. Soc.*, 2010, **5**, 1665–1675.

8 K. Parimal, E. H. Witlicki and A. H. Flood, Interconverting Two Classes of Architectures by Reduction of a Self-Sorting Mixture, *Angew. Chem., Int. Ed.*, 2010, **27**, 4628–4632.

9 E. G. Percástegui, J. Mosquera, T. K. Ronson, A. J. Plajer, M. Kieffer and J. R. Nitschke, Waterproof architectures through subcomponent self-assembly, *Chem. Sci.*, 2019, **7**, 2006–2018.

10 S. Ma, M. M. J. Smulders, Y. R. Hristova, J. K. Clegg, T. K. Ronson, S. Zarra and J. R. Nitschke, Chain-Reaction Anion Exchange between Metal–Organic Cages, *J. Am. Chem. Soc.*, 2013, **15**, 5678–5684.

11 D. Zhang, T. K. Ronson and J. R. Nitschke, Functional Capsules *via* Subcomponent Self-Assembly, *Acc. Chem. Res.*, 2018, **10**, 2423–2436.

12 S.-Z. Li, Y.-X. Wei, Y. Huang and W.-K. Dong, Counteranion-driven self-assembly of di- and tetra-nuclear Zn(II) single-armed salamo-type complexes, *J. Mol. Struct.*, 2022, 133473.

13 C. T. McTernan, T. K. Ronson and J. R. Nitschke, Selective Anion Binding Drives the Formation of AgI8L6 and AgI12L6 Six-Stranded Helicates, *J. Am. Chem. Soc.*, 2021, **2**, 664–670.

14 Y. R. Hristova, M. M. J. Smulders, J. K. Clegg, B. Breiner and J. R. Nitschke, Selective anion binding by a "Chameleon" capsule with a dynamically reconfigurable exterior, *Chem. Sci.*, 2011, **4**, 638–641.

15 C. R. Rice, Metal-assembled anion receptors, *Coord. Chem. Rev.*, 2006, **23**, 3190–3199.

16 A. Thevenet, R. Custelcean, B. A. Moyer and S. Jansone-Popova, Synergistic Self-Assembly of Oxoanions and d-Block Metal Ions with Heteroditopic Receptors into Triple-Stranded Helicates, *Chem.–Eur. J.*, 2020, **26**, 14290–14294.

17 A. Bianchi, K. Bowman-James and E. García-España, Aspects of Anion Coordination from Historical Perspectives, *Anion Coordination Chemistry*, Wiley Online Library, 2011, pp. 1–73.

18 R. A. Begum, S. O. Kang, V. W. Day and K. Bowman-James, Structural Aspects of Anion Coordination Chemistry, *Anion Coordination Chemistry*, Wiley, 2011, pp. 141–225.

19 K. M. Mullen and P. D. Beer, Sulfate anion templation of macrocycles, capsules, interpenetrated and interlocked structures, *Chem. Soc. Rev.*, 2009, **6**, 1701–1713.

20 E. M. Fatila, M. Pink, E. B. Twum, J. A. Karty and A. H. Flood, Phosphate–phosphate oligomerization drives higher order co-assemblies with stacks of cyanostar macrocycles, *Chem. Sci.*, 2018, **11**, 2863–2872.

21 C. R. Benson, C. Maffeo, E. M. Fatila, Y. Liu, E. G. Sheetz, A. Aksimentiev, A. Singharoy and A. H. Flood, Inchworm movement of two rings switching onto a thread by biased

Brownian diffusion represent a three-body problem, *Proc. Natl. Acad. Sci. U. S. A.*, 2018, **38**, 9391–9396.

22 S. Lee, C. H. Chen and A. H. Flood, A pentagonal cyanostar macrocycle with cyanostilbene CH donors binds anions and forms dialkylphosphate [3]rotaxanes, *Nat. Chem.*, 2013, **8**, 704–710.

23 J. Zhao, D. Yang, X.-J. Yang and B. Wu, Anion coordination chemistry: from recognition to supramolecular assembly, *Coord. Chem. Rev.*, 2019, 415–444.

24 J. Sánchez-Quesada, C. Seel, P. Prados, J. de Mendoza, I. Dalcol and E. Giralt, Anion Helicates: Double Strand Helical Self-Assembly of Chiral Bicyclic Guanidinium Dimers and Tetramers around Sulfate Templates, *J. Am. Chem. Soc.*, 1996, **1**, 277–278.

25 S. Li, C. Jia, B. Wu, Q. Luo, X. Huang, Z. Yang, Q.-S. Li and X.-J. Yang, A Triple Anion Helicate Assembled from a Bis(biurea) Ligand and Phosphate Ions, *Angew. Chem., Int. Ed.*, 2011, **25**, 5721–5724.

26 C. Jia, W. Zuo, D. Yang, Y. Chen, L. Cao, R. Custelcean, J. Hostas, P. Hobza, R. Glaser, Y. Y. Wang, X. J. Yang and B. Wu, Selective binding of choline by a phosphate-coordination-based triple helicate featuring an aromatic box, *Nat. Commun.*, 2017, **1**, 938.

27 B. Wu, F. Cui, Y. Lei, S. Li, N. de Sousa Amadeu, C. Janiak, Y.-J. Lin, L.-H. Weng, Y.-Y. Wang and X.-J. Yang, Tetrahedral Anion Cage: Self-Assembly of a $(PO_4)_4L_4$ Complex from a Tris(bisurea) Ligand, *Angew. Chem., Int. Ed.*, 2013, **19**, 5096–5100.

28 H.-Y. Gong, B. M. Rambo, E. Karnas, V. M. Lynch and J. L. Sessler, A 'Texas-sized' molecular box that forms an anion-induced supramolecular necklace, *Nat. Chem.*, 2010, **5**, 406–409.

29 W. Zhao, B. Qiao, J. Tropp, M. Pink, J. D. Azoulay and A. H. Flood, Linear Supramolecular Polymers Driven by Anion-Anion Dimerization of Difunctional Phosphonate Monomers Inside Cyanostar Macrocycles, *J. Am. Chem. Soc.*, 2019, **12**, 4980–4989.

30 W. Zhao, J. Tropp, B. Qiao, M. Pink, J. D. Azoulay and A. H. Flood, Tunable Adhesion from Stoichiometry-Controlled and Sequence-Defined Supramolecular Polymers Emerges Hierarchically from Cyanostar-Stabilized Anion–Anion Linkages, *J. Am. Chem. Soc.*, 2020, **5**, 2579–2591.

31 J. Chen, S. M. A. Fateminia, L. Kacenauskaite, N. Bærentsen, S. Grønfeldt Stenspil, J. Bredehoeft, K. L. Martinez, A. H. Flood and B. W. Laursen, Ultrabright Fluorescent Organic Nanoparticles Based on Small-Molecule Ionic Isolation Lattices, *Angew. Chem., Int. Ed.*, 2021, **17**, 9450–9458.

32 C. R. Benson, L. Kacenauskaite, K. L. VanDenburgh, W. Zhao, B. Qiao, T. Sadhukhan, M. Pink, J. Chen, S. Borgi, C.-H. Chen, B. J. Davis, Y. C. Simon, K. Raghavachari, B. W. Laursen and A. H. Flood, Plug-and-Play Optical Materials from Fluorescent Dyes and Macrocycles, *Chem*, 2020, **8**, 1978–1997.

33 B. Qiao, B. E. Hirsch, S. Lee, M. Pink, C. H. Chen, B. W. Laursen and A. H. Flood, Ion-Pair Oligomerization of Chromogenic Triangulenium Cations with Cyanostar-Modified Anions That Controls Emission in Hierarchical Materials, *J. Am. Chem. Soc.*, 2017, **17**, 6226–6233.

34 Y. Haketa, S. Sasaki, N. Ohta, H. Masunaga, H. Ogawa, N. Mizuno, F. Araoka, H. Takezoe and H. Maeda, Oriented Salts: Dimension-Controlled Charge-by-Charge Assemblies from Planar Receptor–Anion Complexes, *Angew. Chem., Int. Ed.*, 2010, **52**, 10079–10083.

35 N. Fumoto, Y. Haketa, H. Tanaka, N. Yasuda and H. Maeda, π-Electronic Ion-Pairing Assemblies of Deprotonation-Induced Anions, *Org. Lett.*, 2021, **10**, 3897–3901.

36 C. Jia, B. P. Hay and R. Custelcean, *De Novo* Structure-Based Design of Ion-Pair Triple-Stranded Helicates, *Inorg. Chem.*, 2014, **7**, 3893–3898.

37 A. J. McConnell, A. Docker and P. D. Beer, From Heteroditopic to Multitopic Receptors for Ion-Pair Recognition: Advances in Receptor Design and Applications, *ChemPlusChem*, 2020, **8**, 1824–1841.

38 A. J. McConnell and P. D. Beer, Heteroditopic Receptors for Ion-Pair Recognition, *Angew. Chem., Int. Ed.*, 2012, **21**, 5052–5061.

39 S. K. Kim and J. L. Sessler, Ion pair receptors, *Chem. Soc. Rev.*, 2010, **10**, 3784–3809.

40 M. Alfonso, A. Tárraga and P. Molina, Pyrrole, imidazole, and triazole derivatives as ion-pair recognition receptors, *Tetrahedron Lett.*, 2016, **29**, 3053–3059.

41 H.-W. Schmidt and F. Würthner, A Periodic System of Supramolecular Elements, *Angew. Chem., Int. Ed.*, 2020, **23**, 8766–8775.

42 D. Asil, J. A. Foster, A. Patra, X. de Hatten, J. del Barrio, O. A. Scherman, J. R. Nitschke and R. H. Friend, Temperature- and Voltage-Induced Ligand Rearrangement of a Dynamic Electroluminescent Metallopolymer, *Angew. Chem., Int. Ed.*, 2014, **32**, 8388–8391.

43 J. R. Nitschke, Construction, substitution, and sorting of metallo-organic structures *via* subcomponent self-assembly, *Acc. Chem. Res.*, 2007, **40**, 103–112.

44 X.-Q. Guo, L.-P. Zhou, S.-J. Hu, L.-X. Cai, P.-M. Cheng and Q.-F. Sun, Hexameric Lanthanide–Organic Capsules with Tertiary Structure and Emergent Functions, *J. Am. Chem. Soc.*, 2021, **16**, 6202–6210.

45 Y. Domoto, M. Abe and M. Fujita, A Highly Entangled (M3L2) 8 Truncated Cube from the Anion-Controlled Oligomerization of a π-Coordinated M3L2 Subunit, *J. Am. Chem. Soc.*, 2021, **23**, 8578–8582.

46 A. Dhara, T. Sadhukhan, E. G. Sheetz, A. H. Olsson, K. Raghavachari and A. H. Flood, Zero-Overlap Fluorophores for Fluorescent Studies at Any Concentration, *J. Am. Chem. Soc.*, 2020, **28**, 12167–12180.

47 F. J. Rizzuto, L. K. S. von Krbek and J. R. Nitschke, Strategies for binding multiple guests in metal–organic cages, *Nat. Rev. Chem.*, 2019, **4**, 204–222.

48 D. J. Gorin and F. D. Toste, Relativistic effects in homogeneous gold catalysis, *Nature*, 2007, **446**, 395–403.

49 A. Y. Sokolov and O. V. Sizova, Quantum-chemical study of trans influence in gold(I) linear complexes, *Russ. J. Gen. Chem.*, 2010, **7**, 1223–1231.

50 K. H. Hopmann and A. Bayer, Enantioselective imine hydrogenation with iridium-catalysts: reactions, mechanisms and stereocontrol, *Coord. Chem. Rev.*, 2014, **268**, 59–82.

51 Y. Yang, L. Eberle, F. F. Mulks, J. F. Wunsch, M. Zimmer, F. Rominger, M. Rudolph and A. S. K. Hashmi, Trans Influence of Ligands on the Oxidation of Gold(I) Complexes, *J. Am. Chem. Soc.*, 2019, **43**, 17414–17420.

52 B. Qiao, G. M. Leverick, W. Zhao, A. H. Flood, J. A. Johnson and Y. Shao-Horn, Supramolecular Regulation of Anions Enhances Conductivity and Transference Number of Lithium in Liquid Electrolytes, *J. Am. Chem. Soc.*, 2018, **35**, 10932–10936.

53 M. Brookhart, B. Grant and A. F. Volpe, $[(3,5\text{-}(CF_3)_2C_6H_3)4B]\text{-}[H(OEt_2)2]^+$: a convenient reagent for generation and stabilization of cationic, highly electrophilic organometallic complexes, *Organometallics*, 1992, **11**, 3920–3922.

54 A. Macchioni, Ion Pairing in Transition-Metal Organometallic Chemistry, *Chem. Rev.*, 2005, **6**, 2039–2074.

55 C. R. Benson, E. M. Fatila, S. Lee, M. G. Marzo, M. Pink, M. B. Mills, K. E. Preuss and A. H. Flood, Extreme Stabilization and Redox Switching of Organic Anions and Radical Anions by Large-Cavity, CH Hydrogen-Bonding Cyanostar Macrocycles, *J. Am. Chem. Soc.*, 2016, **45**, 15057–15065.

56 B. E. Hirsch, K. P. McDonald, B. Qiao, A. H. Flood and S. L. Tait, Selective Anion-Induced Crystal Switching and Binding in Surface Monolayers Modulated by Electric Fields from Scanning Probes, *ACS Nano*, 2014, **10**, 10858–10869.

57 E. M. Fatila, E. B. Twum, A. Sengupta, M. Pink, J. A. Karty, K. Raghavachari and A. H. Flood, Anions Stabilize Each Other inside Macrocyclic Hosts, *Angew. Chem., Int. Ed.*, 2016, **45**, 14057–14062.

58 D. Asil, J. A. Foster, A. Patra, X. de Hatten, J. del Barrio, O. A. Scherman, J. R. Nitschke and R. H. Friend, Temperature- and Voltage-Induced Ligand Rearrangement of a Dynamic Electroluminescent Metallopolymer, *Angew. Chem., Int. Ed.*, 2014, **32**, 8388–8391.

59 E. Sheetz, Z. Zhang, A. Marogil, M. Che, M. Pink, V. Carta, K. Raghavachari and A. H. Flood, High-fidelity recognition of organotrifluoroborate anions ($R\text{–}BF^{3-}$) as designer guest molecules, *Chem.–Eur. J.*, 2022, **60**, e202201584.

60 E. M. Fatila, E. B. Twum, J. A. Karty and A. H. Flood, Ion Pairing and Co-facial Stacking Drive High-Fidelity Bisulfate Assembly with Cyanostar Macrocyclic Hosts, *Chem.–Eur. J.*, 2017, **44**, 10652–10662.

61 R. E. Fadler, A. Al Ouahabi, B. Qiao, V. Carta, N. F. Konig, X. Gao, W. Zhao, Y. Zhang, J. F. Lutz and A. H. Flood, Chain Entropy Beats Hydrogen Bonds to Unfold and Thread Dialcohol Phosphates inside Cyanostar Macrocycles To Form [3]Pseudorotaxanes, *J. Org. Chem.*, 2021, **6**, 4532–4546.

62 R. E. Fadler, A. Al Ouahabi, B. Qiao, V. Carta, N. F. König, X. Gao, W. Zhao, Y. Zhang, J.-F. Lutz and A. H. Flood, Chain Entropy Beats Hydrogen Bonds to Unfold and Thread Dialcohol Phosphates inside Cyanostar Macrocycles To Form [3]Pseudorotaxanes, *J. Org. Chem.*, 2021, **6**, 4532–4546.

63 K. Maršálek and V. Šindelář, Monofunctionalized Bambus[6]urils and Their Conjugates with Crown Ethers for Liquid–Liquid Extraction of Inorganic Salts, *Org. Lett.*, 2020, **4**, 1633–1637.

64 T. Lizal and V. Sindelar, Bambusuril Anion Receptors, *Isr. J. Chem.*, 2018, **3–4**, 326–333.

65 M. A. Yawer, V. Havel and V. Sindelar, A Bambusuril Macrocycle that Binds Anions in Water with High Affinity and Selectivity, *Angew. Chem., Int. Ed.*, 2015, **1**, 276–279.

66 V. Havel, J. Svec, M. Wimmerova, M. Dusek, M. Pojarova and V. Sindelar, Bambus[*n*]urils: a new family of macrocyclic anion receptors, *Org. Lett.*, 2011, **15**, 4000–4003.